Ultrafast second-Stokes diamond Raman laser

Michelle Murtagh,[1,2] Jipeng Lin,[1] Johanna Trägårdh,[2] Gail McConnell[2] and David J. Spence[1,*]

[1]*MQ Photonics, Department of Physics and Astronomy, Macquarie University, NSW 2109, Australia*
[2]*Centre for Biophotonics, Strathclyde Institute for Pharmacy and Biomedical Sciences, University of Strathclyde, G4 0RE, UK*
*david.spence@mq.edu.au

Abstract: We report a synchronously-pumped femtosecond diamond Raman laser operating with a tunable second-Stokes output. Pumped using a mode-locked Ti:sapphire laser at 840-910 nm with a duration of 165 fs, the second-Stokes wavelength was tunable from 1082 - 1200 nm with sub-picosecond duration. Our results demonstrate potential for cascaded Raman conversion to extend the wavelength coverage of standard laser sources to new regions.

OCIS codes: (140.3550) Lasers, Raman; (140.3560) Lasers, ring; (140.3580) Lasers, solid-state; (140.7090) Ultrafast lasers.

_____

References and links

1. W. R. Zipfel, R. M. Williams, and W. W. Webb, "Nonlinear magic: multiphoton microscopy in the biosciences," Nature biotechnology **21**, 1369-1377 (2003).
2. L.-C. Cheng, N. G. Horton, K. Wang, S.-J. Chen, and C. Xu, "Measurements of multiphoton action cross sections for multiphoton microscopy," Biomedical Optics Express **5**, 3427-3433 (2014).
3. J. Tragadh, G. Robb, R. Amor, W. B. Amos, J. Dempster, and G. McConnell, "Exploration of the two-photon excitation spectrum of fluorescent dyes at wavelengths below the range of the Ti:Sapphire laser," Journal of Microscopy **259**, 210-218 (2015).
4. W. Zheng, D. Li, Y. Zeng, Y. Luo, and J. Y. Qu, "Two-photon excited hemoglobin fluorescence," Biomedical Optics Express **2**, 9 (2011).
5. G. C. R. Ellis-Davies, "Caged compounds: photorelease technology for control of cellular chemistry and physiology," Nature methods **4**, 619-628 (2007).
6. D. T. Reid, J. Sun, T. P. Lamour, and T. I. Ferreiro, "Advances in ultrafast optical parametric oscillators," Laser Physics Letters **8**, 8-15 (2011).
7. E. Granados, H. M. Pask, E. Esposito, G. McConnell, and D. J. Spence, "Multi-wavelength, all-solid-state, continuous wave mode locked picosecond Raman laser," Optics Express **18**, 5289-5294 (2010).
8. E. Granados, H. M. Pask, and D. J. Spence, "Synchronously pumped continuous-wave mode-locked yellow Raman laser at 559 nm," Optics Express **17**, 6 (2009).
9. A. M. Warrier, J. Lin, H. M. Pask, R. P. Mildren, D. W. Coutts, and D. J. Spence, "Highly efficient picosecond diamond Raman laser at 1240 and 1485 nm," Optics Express **22**, 3325 (2014).
10. M. Murtagh, J. Lin, R. P. Mildren, G. McConnell, and D. J. Spence, "Efficient diamond Raman laser generating 65 fs pulses," Optics express **23**, 15504-15513 (2015).
11. M. Murtagh, J. Lin, R. P. Mildren, and D. J. Spence, "Ti:sapphire-pumped diamond Raman laser with sub-100-fs pulse duration," Optics Letters **39**, 2975-2978 (2014).
12. J. Lin and D. Spence, "25.5 fs dissipative-soliton diamond Raman laser," Optics Letters (to be published).
13. P. Farinello, F. Pirzio, X. Zhang, V. Petrov, and A. Agnesi, "Efficient picosecond traveling-wave Raman conversion in a SrWO4 crystal pumped by multi-Watt MOPA lasers at 1064 nm," Appl. Phys. B **120**, 731-735 (2015).
14. R. P. Mildren, A. Sabella, O. Kitzler, D. J. Spence, and A. M. McKay, "Diamond Raman Laser Design and Performance," in *Optical Engineering of Diamond* (2013), pp. 239-276.
15. D. Churin, J. Olson, R. A. Norwood, N. Peyghambarian, and K. Kieu, "High-power synchronously pumped femtosecond Raman fiber laser," Optics Letters **40**, 2529-2532 (2015).
16. T. B. Tasoltan, E. D. Maxim, I. I. Lyudmila, N. S. Sergei, M. Jelínek, V. Kubeček, and H. Jelínková, "Four-wave-mixing generation of SRS components in BaWO 4 and SrWO 4 crystals under picosecond excitation," Quantum Electronics **43**, 616 (2013).

17. T.-M. L. K. Wang, J. Wu, N. G. Horton, C. P. Lin and C. Xu, "Three-color femtosecond source for simultaneous excitation of three fluorescent proteins in two-photon fluorescence microscopy," Biomedical Optics Express **3**(2012).
_____

1. Introduction

Ultrafast lasers play a crucial role in biological imaging; for example two-photon microscopy allows images of live tissue to be taken in three dimensions using long excitation wavelengths, giving a large penetration depth and low cell damage (in particular compared to excitation with wavelengths at the blue end of the visible spectrum). The combination of a large number of different possible fluorophores, as well as different available nonlinear imaging methods (such as SHG and three-photon excitation), mean that laser pulses are required all the way from the blue to the near-infrared spectral region. Ti:sapphire lasers are the most commonly used lasers, allowing coverage of the range 680 - 1080 nm, but access to a broader wavelength range is desirable: for example, access to still longer wavelengths allows two-photon imaging of red excited fluorophores and three-photon imaging of green excited fluorophores [1, 2]; access to shorter wavelengths allows efficient two-photon microscopy of many fluorophores [3] and endogenous chromophores such as NADH and FAD [4], and photolysis of short-wavelength activated compounds such as caged IP3 [5].

Conversion of standard ultrafast lasers sources such as Ti:sapphire lasers to new spectral ranges can be a cost-effective route to access new wavelengths. Synchronously-pumped optical parametric oscillators are well-established for the conversion of femtosecond laser pulses [6] and can reach a wide range of wavelengths. Stimulated Raman scattering (SRS) is an alternative nonlinear optical process that can shift the wavelength of a conventional laser to one or more longer wavelengths. Conversion of picosecond pulsed laser oscillators using SRS in crystals has been demonstrated for first- and second-Stokes output in the visible and infrared [7-9]. This has been extended into the femtosecond regime for first-Stokes output, generating pulses as short as 25.5 fs [10-12]. In this paper, we investigate the characteristics of a second-Stokes diamond Raman laser synchronously pumped by a fs-pulsed Ti:sapphire laser. This second-Stokes laser is tunable from 1082 - 1201 nm when pumped in the range $840 - 910$ nm. In principle, using the full Ti:sapphire pump tuning range and frequency doubling, such a laser could reach all wavelengths from 380 to 1510 nm.

2. Experimental setup

The experimental set up for our synchronously-pumped second-Stokes diamond Raman laser is shown in Fig.1. Synchronous pumping is required to get efficient conversion of the nanojoule-scale pulses available from typical ultrafast oscillators, in contrast to microjoule-scale pulses that allow for single-pass SRS [13]. Diamond was chosen as the Raman material because of its high gain coefficient and relatively large Raman shift (1332 cm^{-1}) compared to most other Raman crystals, in addition to its potential for high average power operation. The diamond crystal (Type IIa, CVD-grown, 8 mm-long) had broadband AR-coatings from 796 nm - 1200 nm. The Ti:sapphire pump laser operating between 840 and 910 nm generated 165 fs pulses with a pulse repetition frequency of 80 MHz. From the measured bandwidth of 6 nm, we can estimate a 124 fs transform-limited pump pulse, and we confirmed that the pump pulses were slightly positively chirped. The pump beam was polarized parallel to the $\langle 111 \rangle$ axis of the diamond crystal to access the highest Raman gain, and the Stokes output was polarized parallel to the pump as expected [14]. The pump beam was focused through the input mirror M1 into the centre of the diamond crystal.
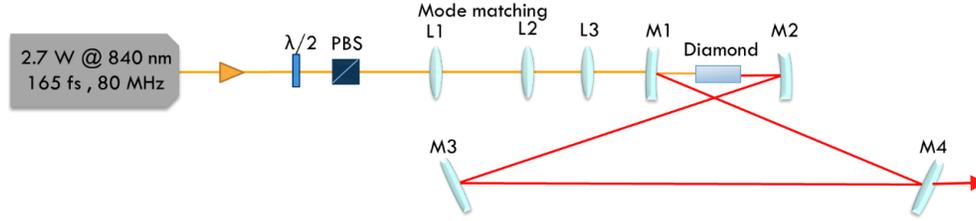
Fig. 1. Layout of experiment setup. λ/2: half-wave plate; PBS: polarizing beam splitting cube; L1, L2: mode matching lenses; L3: focusing lens; M1, M2: mirrors with ROC of 200 mm, M3, M4: plane mirrors.

The Raman laser was configured as a ring cavity, consisting of two concave mirrors (M1 and M2, radius of curvature (ROC) of 200 mm) and two plane mirrors (M3 and M4). Table 1 presents a summary of the cavity mirror coatings. For a second-Stokes laser, we want to have a high-Q cavity for the first-Stokes field that we expect to center between 946 – 1046 nm for this pump range. Mirror M1 and M2 had T=98 – 99% for 830-910 nm and R>99.9% for 920 – 1300 nm. M3 had R>99.9% for 920 – 1300 nm; output coupler (OC) M4 had a roughly constant transmission of T≈30% for 1050 – 1300 nm. A separation of approximately 206 mm between M1 and M2 produced a TEM_{00} mode of 25 µm radius at the centre of the diamond. The cavity round-trip time was closely matched to the pump laser interpulse period by translation of mirror M4. We characterized the laser by measuring the spectra, pulse duration and pump-to-Stokes power conversion. These experimental results are presented below.

Table 1. Summary of mirror coating reflectivity.

	Pump region: 830-910 nm	First Stokes region: 920-1050 nm	Second Stokes region: 1050-1220 nm
M1	T = 98 – 99%	R > 99.9%	R > 99.9%
M2	T = 99.9%	R > 99.9%	R > 99.9%
M3	T = 99.9%	R > 99.9%	R > 99.9%
M4 (OC)	T = 99.9%	R > 99.9%	T ≈ 30 %

3. Results

3.1 Laser power and spectrum

With the pump laser tuned to 840 nm and the second-Stokes at 1082 nm, we measured a pump-to-Stokes laser slope efficiency of 20%, as shown in Fig. 2. The second-Stokes laser threshold was 0.675 W, and 400 mW output at 1082 nm was obtained at the maximum pump power of 2.7 W. The first-Stokes laser threshold measured as 0.5 W.

Figure 3 shows the first- and second-Stokes spectra measured at the maximum pump power. The first- and second-Stokes spectra are plotted on separate wavelength axes, aligned so that wavelengths shifted by the diamond Raman shift of 1332 cm^{-1} remain overlapped. The first-Stokes spectrum had a central wavelength of 945 nm, and was broadened compared to the pump (which had 6 nm width, centered at 840 nm), displaying two sharp peaks at both blue and red ends of the spectrum. The first-Stokes spectrum spanned approximately 30 nm from peak-to-peak (bottom x-axis for Fig. 3). This spectrum is similar to that observed for equivalent first-Stokes lasers [10-12] owing to strong self-phase modulation and dispersion in the cavity that leads to a chirped and broadened first-Stokes pulse. The pulse formed by the balance between these two effects and the gain-narrowing associated with the Raman amplification can be described as a dissipative soliton [15].
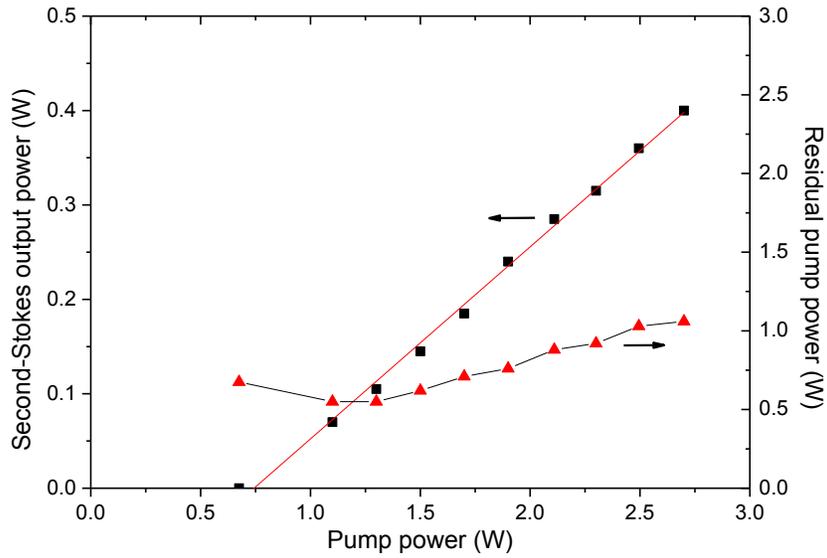
Fig. 2. The average Stokes output power vs. pump power (black squares), showing a maximum output of 400 mW and a 20% slope efficiency. The right-hand axis shows the residual pump power (red triangles) after passing through the diamond crystal and mirror M2.
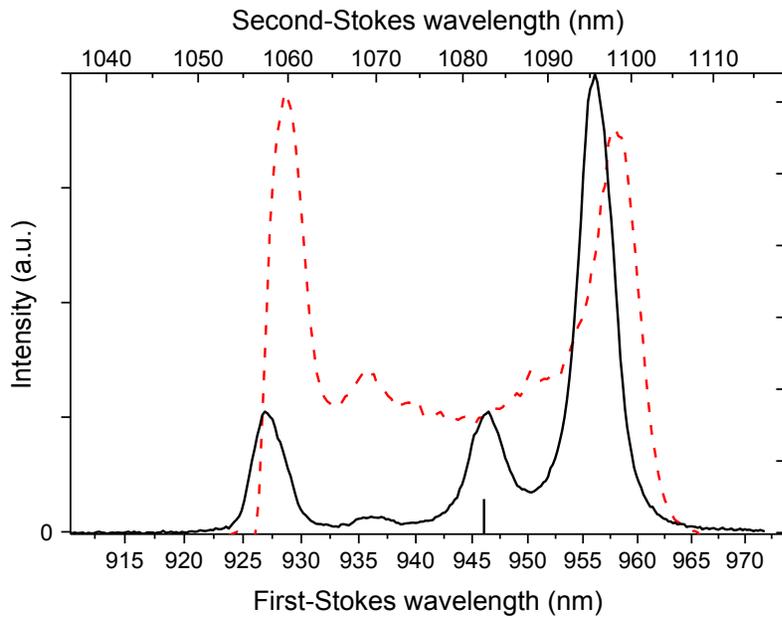

Fig. 3. Comparison of first- (bottom x-axis, dashed red) and second-Stokes (top x-axis, black) spectra at a pump wavelength of 840 nm. Both x-axes are linear in frequency space, and shifted so that each first-Stokes wavelength aligns with the corresponding second-Stokes wavelength for a diamond Raman shifted of 1332 cm^{-1}. The 946 nm wavelength associated with a Raman shift of the pump center wavelength of 840 nm is marked.

The dissimilarity between the pump and first-Stokes spectra is in contrast to the similarity between the first- and second-Stokes: The second-Stokes spectrum is closer to a spectrally-shifted copy of the first-Stokes spectrum. The additional spectral power near the exact second-Stokes central shifted wavelength seems to correspond to the pump linewidth and may be due to four-wave mixing of pump and first-Stokes. Since we are not strongly resonating the second-Stokes field, it does not accumulate cross-phase modulation from the intense first-Stokes field, and so we expect little additional broadening of the spectrum.

We measured the intensity autocorrelation (using SHG) of the second-Stokes pulse. We have assumed a sech^2 pulse shape to obtain a pulse width of 910 fs at 1082 nm directly from the Raman laser. Using an dispersion compensating prism-pair (N-SF14 glass) with 0.6 m prism separation we compressed the second-Stokes pulse to get a slightly shorter pulse duration of 845 fs. This lack of significant compression indicates that the second-Stokes spectrum phase is not a simple chirp, unlike for first-Stokes lasers of this type [10-12]. A typical autocorrelation trace for the compressed second-Stokes output is shown in Fig. 4. It shows no substantial pedestal, and the small peak around zero delay indicates some weak intensity structure on a 100-fs timescale.
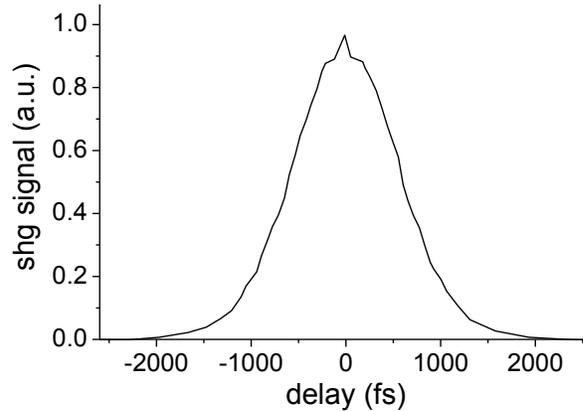

Fig. 4. Second-harmonic generation (SHG) autocorrelation measurement for the compressed second Stokes pulse, corresponding to a retrieved pulse duration of 845 fs.

3.2 Tuning the second-Stokes output wavelength

We studied experimentally the output power for the second-Stokes laser as a function of input pump wavelength. We tuned the pump laser from 840-910 nm producing second-Stokes output between 1082-1201 nm. This tuning range refers to the location of the central feature of the second Stokes spectrum, which is consistently two Raman shifts from the pump center wavelength. Figure 5 shows the second-Stokes and pump power as a function of pump wavelength. For each data point, the laser was optimized in terms of cavity length, mode overlap, and the position of the diamond. The second-Stokes power and pump power decreased together as the pump wavelength was increased, with the second-Stokes laser efficiency is largely unchanged below 890 nm. This insensitivity to wavelength of the efficiency is as expected, with the Raman process having no phase-matching consideration, and weak dependence of gain on wavelength [14]. The steeper drop in the second-Stokes output for pump wavelengths greater than 890 nm was due to the cavity input mirror (M1) starting to reflect an increasing fraction of the pump power.
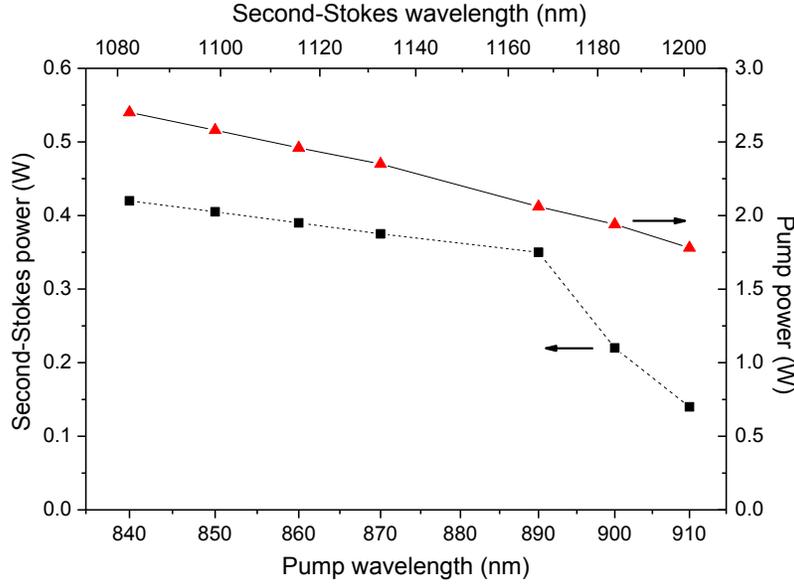
Fig. 5. Input pump power (red triangles) and second-Stokes output power (black squares) as a function of pump wavelength. The corresponding second-Stokes central wavelength is shown on the top axis.

4. Discussion

We now compare this result to previous work on picosecond second-Stokes lasers to understand the additional complexities involved in our experiment. There are two previous ultrafast cascaded synchronously-pumped crystalline Raman lasers, each working differently.

Second-Stokes output at 1485 nm with 10 ps pulse duration was observed with a maximum of 1 W of second-Stokes average power from 4.8 W pump power from a 1064 nm, 15 ps laser [9]. This corresponds to a 21% conversion efficiency. In this experiment diamond was the Raman active medium and the cavity mirrors were highly reflective only at the first-Stokes wavelength 1240 nm. The second-Stokes was very weakly resonated with just 0.02% of light completing each round-trip. The generation of the second-Stokes was in this case seeded by parametric four-wave mixing (FWM) between the pump, first- and second-Stokes fields, where two first-Stokes photons combine to generate one pump and one second-Stokes photon. This phase-mismatched process generated a weak seed pulse for single-pass Raman amplification. Such FWM-seeding is common in Raman generators, e.g. in [16], where second- and third-Stokes generation was achieved using short crystals.

An alternative method is to cascade to higher Stokes orders using high-Q resonators for all Stokes fields. Pumped by a 532 nm laser with 28 ps pulse duration and 7 W of average power, 2.5 W of 559 nm first-Stokes output was obtained with 6.5 ps pulse duration, and 1.4 W of 589 nm second-Stokes output with 5.5 ps pulse duration [7]. In this work, non-resonated second-Stokes was not observed, possibly since the FWM phase mismatch is worse at these wavelengths. Due to the temporal walk-off between the pulses through the Raman crystal, different cavity lengths are ideally required to synchronize the pump with the first- and second-Stokes pulses in the absence of gain. By splitting the first- and second-Stokes cavity fields onto different end mirrors using an intracavity prism pair, the first- and second-Stokes cavity lengths were independently controlled by adjusting the different end mirrors in order to optimize the laser.

In the present laser using shorter 165 fs pump pulses, we also did not observe single-pass generation of second-Stokes when using mirrors that did not resonate the second Stokes. For the results presented here, the first- and second-Stokes fields use the same mirrors, and so the cavity lengths are constrained to be equal for the two fields. For a pump wavelength of 840 nm, the difference in transit time of the first-Stokes 946 nm pulse and the second-Stokes 1082 nm pulse in 8 mm of diamond is 310 fs; this means that the second-Stokes cavity should ideally be 93 μm shorter than the first-Stokes cavity to keep the fields synchronised. Since the laser operates in steady-state, the gain for the second-Stokes must reshape the pulse on each round trip to effectively delay it by 310 fs. Such significant reshaping requires large gain, provided by the strongly-resonated first-Stokes field. We suggest that the strong reshaping that is required by the effective cavity length error prevents the development of a coherent phase across the pulse, which is the likely reason for the long, uncompressible pulses observed here. Similar noise-like pulses in synchronous fibre lasers have been observed for large cavity length errors [15]. While the present laser is fairly efficient, we propose the future possibility of resonating the first- and second-Stokes fields separately in an attempt to improve conversion efficiency as well as generating a compressible second-Stokes pulse.

This Raman approach can extend the wavelength coverage of any available ultrafast laser source, and the Raman laser can be continuously tuned by tuning the pump laser. We have demonstrated this tunability using a Ti:sapphire pump laser; however, the method can be applied to a wide range of picosecond or femtosecond sources to be found in laboratories. For example, we could use Yb fiber or VECSEL lasers as pump sources. Figure 6 shows output first- and second-Stokes output wavelengths for diamond Raman lasers using various pump wavelengths.
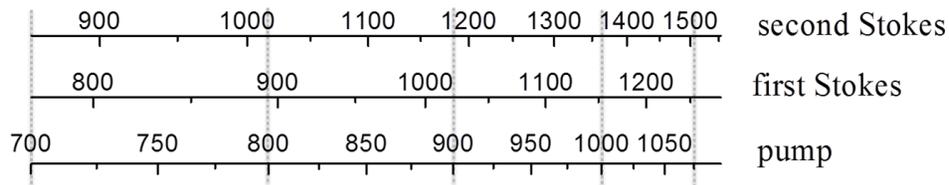

Fig. 6. Output wavelengths from a diamond Raman laser using various pump wavelengths.

5. Conclusion

We have presented a diamond Raman laser with a tunable second-Stokes output, spanning the wavelength range 1082-1201 nm. Using 840 nm pump wavelength, we obtained 400 mW of second-Stokes average power output at 1082 nm, with 20% slope efficiency, and a pulse duration of 910 fs without compression, and 845 fs with compression.

Developing Raman lasers to output first-, second- and higher-order Stokes wavelengths allows the generation of a wide range of wavelengths from a single base system for applications, for example in nonlinear microscopy. Another possible advantage is that the lasers can simultaneously have multiple wavelengths output collinearly from the cavity, which could be used for simultaneous imaging of a multiple-labelled samples such as in [17].

Acknowledgments